Jianfeng Sun
Department of Mechanical and Industrial Engineering, Northeastern University, Boston, MA 02115

Sinan Müftü
Department of Mechanical and Industrial Engineering, Northeastern University, Boston, MA 02115

April Z. Gu[1]
Department of Civil and Environmental Engineering, Northeastern University, Boston, MA 02115

Kai-Tak Wan[2]
Department of Mechanical and Industrial Engineering, Northeastern University, Boston, MA 02115
e-mail: ktwan@coe.neu.edu

Intersurface Adhesion in the Presence of Capillary Condensation

An elastic sphere adheres to a rigid substrate in the presence of moisture. The adhesion–detachment trajectory is derived based on the Hertz contact theory that governs the contact mechanics and Laplace–Kelvin equation that governs the water meniscus at the interface. The intersurface attraction is solely provided by the Laplace pressure within the meniscus. Interrelation between the applied load, contact radius, and approach distance is derived based on a force balance. The resulting "pulloff" force to detach the sphere exceeds the critical load in the Derjaguin–Muller–Toporov (DMT) limit which only holds at saturated moisture. The new model accounts for the finite size of water molecules that is missing in virtually all classical models.
[DOI: 10.1115/1.4039621]

1 Introduction

Adhesion of an elastic sphere onto another sphere or a rigid substrate is ubiquitous in many branches of science and technology such as colloidal particles, storage and transportation of glass powder, and micro-electromechanical systems especially when the typical dimension shrinks to submicron scale [1–3]. Exposure to moist air leads to meniscus formation at the contact interface and could post serious problems of operation hindrance and reliability.

Meticulous experimental work conducted by Christenson [4,5], Maugis and Gauthier-Manuel [6], and Xu et al. [7], and theoretical framework constructed by Fogden and White [8], and Grobelny et al. [9] demonstrated the effect of moisture on adhesion. In a relatively dry environment, the inevitable meniscus shrinks to a small dimension, and the resulting short range Laplace pressure leads to the Johnson–Kendall–Roberts (JKR) limit. Close to saturated moisture, the meniscus grows to such a large extent that adhesion mechanics approaches the Derjaguin–Muller–Toporov (DMT) limit. Wan and Lawn [10] and Wan et al. [11] investigated adhesion of two noninteracting elastic cantilevers in the presence of meniscus, and found that the critical energy release rate is twice the surface tension of water as if the crack front is right at the meniscus. The intermediate range of relative humidity falls into the JKR–DMT transition and is accounted for by the Tabor's parameter [12]. In such classical work, the "pulloff" force leading to spontaneous detachment is taken to be $F^* = -\chi \times \pi R \times 2\gamma \cos\theta$, where R is the sphere radius, γ is the surface tension of water, θ is the contact angle at meniscus–solid interface, and χ is a numerical constant $\chi_{JKR} \le \chi \le \chi_{DMT}$ with $\chi_{JKR} = 3/2$ and $\chi_{DMT} = 2$. Therefore, F^* is a monotonic increasing function of relative humidity approaching the JKR and DMT limits in the extremes. Zeng and Streator [13] and Xue and Polycarpou [14,15] started from a long-range intersurface attraction and derived the sphere deformation. The numerical approach interestingly suggests that F^* is a monotonically decreasing function of humidity as it approaches the DMT limit.

In this paper, we will build an alternative model based on the Hertz contact theory [2] and cohesive zone model [16], rather similar to the DMT model. We will first present the theory and results, leaving the discussion and comparison with the classical models to Sec. 4. In the absence of moisture, the intrinsic intersurface forces such as van der Waals are present, but such interactions are taken as the baseline or ignored hereafter to avoid unnecessary mathematical complications. The total force acting on the sphere, therefore, becomes the sum of the applied load and the Laplace pressure within the meniscus. The compressive stress distribution within the contact and the deformed geometry strictly follow the classical Hertz contact theory [17]. The Dugdale–Barenblatt–Maugis cohesive zone model is adapted where the disjoining pressure is taken to be constant over a finite range determined by the Laplace–Kelvin equation [10,11,16,18]. The measurable relations of applied load, contact radius, and approach distance are derived.

2 Theory

A compressive load, F, is applied to an elastic sphere with radius R, elastic modulus, E, and Poisson's ratio, ν, resulting in an approach distance, δ, and contact radius, a. In the absence of adhesion, the classical Hertz contact theory [17] gives the interrelation of (F, a, δ)

$$\delta = \frac{a^2}{R} \tag{1}$$

$$F = \frac{4}{3}\left(\frac{E}{1-\nu^2}\right)\frac{a^3}{R} \tag{2}$$

and the axisymmetric deformed profile $z(r)$, or equivalently, intersurface separation at r

[1]Present address: Civil and Environmental Engineering, Cornell University, Ithaca, NY 14853.
[2]Corresponding author.
Contributed by the Applied Mechanics Division of ASME for publication in the Journal of Applied Mechanics. Manuscript received February 6, 2018; final manuscript received March 11, 2018; published online April 4, 2018. Editor: Yonggang Huang.

$$z(r) = \frac{r^2}{2R} - \delta + \frac{a^2}{\pi R}\left\{\sqrt{\left(\frac{r}{a}\right)^2 - 1} + \left[2 - \left(\frac{r}{a}\right)^2\right]\sin^{-1}\frac{a}{r}\right\} \quad \text{for } r > a \tag{3}$$

At equilibrium, the external load is balanced by the repulsive reaction force, $F_H = F$, governed by Eq. (2). In the presence of a general intersurface interaction potential $\phi(z)$, a disjoining pressure $p = d\phi(z)/dz$ arises at the sphere–substrate interface, and the total adhesion force acting on the sphere becomes

$$F_{ad}(a) = \int_a^\infty \frac{d\phi(z)}{dz} \times 2\pi r dr \tag{4}$$

Here, F_{ad} is taken as an addition to the applied load, F, while Eqs. (1)–(3) remain valid. The net applied load to maintain a force balance is, therefore, given by

$$F = F_H(a) - F_{ad}(a) \tag{5}$$

The Dugdale–Barenblatt–Maugis approximation requires the disjoining pressure to be uniform, p^*, with a range, z^*, over a cohesive zone immediately outside the contact circle (Fig. 1), such that

$$p(z) = \begin{cases} 0 & \text{for } z < z_0 \quad \text{and} \quad r < a \\ p* & \text{for } z_0 \le z \le z* \quad \text{and} \quad a < r < a_1 \\ 0 & \text{for } z > z* \quad \text{and} \quad r > a_1 \end{cases} \tag{6}$$

where z_0 is the equilibrium sphere–substrate separation to account for the finite dimension of molecular planes. The annular cohesive zone is bounded by $a < r \le a_1$ with $z(r = a_1) = z^*$. Substituting Eq. (6) into Eq. (4), the effective adhesion force becomes

$$F_{ad} = p* \times \pi\left(a_1^2 - a^2\right) \tag{7}$$

with the interfacial adhesion energy given by $\gamma = p^* \times (z^* - z_0) \approx p^* \times z^*$, since $z^* \gg z_0$. It is apparent that a_1 depends on both z^* which depends on the interface chemistry and $z(r)$ which depends on the elastic deformation. The measurable relations, $a(F)$ and $a(\delta)$, can then be solved based on Eqs. (1)–(7).

When the sphere is exposed to a humid environment, water vapor condenses at the contact edge forming a meniscus at the cleft. The negative Laplace pressure in the meniscus now serves as the only intersurface attraction and is uniform within the cohesive zone given by $p^* = \gamma/r_k$, with γ the surface tension (or, equivalently, surface energy) of water. Rather than accounting for the sophisticated principal curvatures of the meniscus and the geometry of the deformed sphere, the force range is taken to be approximately the meniscus diameter or twice the Kelvin radius [10], r_k, or

$$z^* = 2r_k \cos\theta = \frac{2v_m\gamma\cos\theta}{kT\ln(1/\mathrm{RH})} \approx \frac{2v_m\gamma}{kT\ln(1/\mathrm{RH})} \tag{8}$$

with a contact angle $\theta \approx 0$ deg, molecular volume of water v_m, Boltzmann's constant k, temperature $T \approx 300$ K, and relative humidity RH. At the saturation limit (RH $\approx$ 100%), $p^* \to 0$ and $z^* \to \infty$. Without the loss of generality, θ is taken to be zero hereafter. In case of a nonzero θ, all γ term will be replaced by $\gamma\cos\theta$. In dry conditions with RH = 0%, $p^* \to \infty$ and $z^* \to 0$. Using Eq. (7), the adhesive force is given by

$$F_{ad} = \frac{kT\ln(1/RH)}{v_m} \times \pi\left(a_1^2 - a^2\right) \tag{9}$$

The relation (F, a, δ) can then be found numerically by substituting Eqs. (8) and (9) into Eqs. (1)–(7).

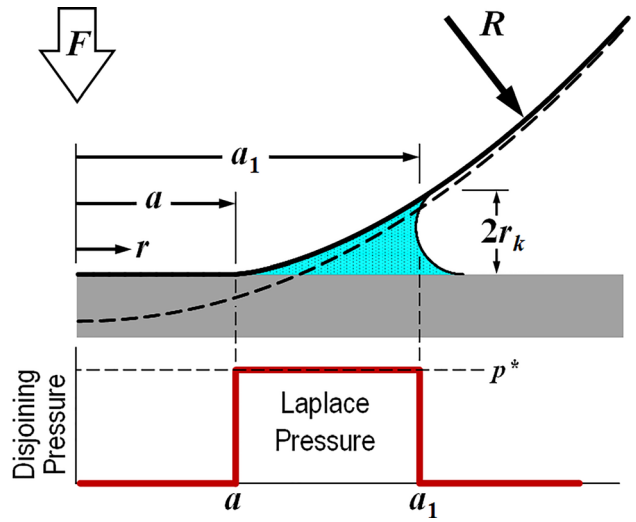

Fig. 1 An elastic solid is deformed from a spherical geometry (*dashed curve*) into Hertz profile (*solid curve*). The uniform Laplace pressure bounded by the meniscus exerts traction on the sphere in addition to the applied load.

3 Results

Figure 2(*a*) shows $a(F)$ for a range of RH for a sphere with $E = 1.0$ GPa. For RH = 5%, the detachment trajectory follows path ABCDO (dark curve). At A when $F = 0$, a nonzero contact radius is expected. Increasing tensile load ($F < 0$) reduces the contact circle along ABC until the sphere spontaneously detaches from the substrate or "pulloff" at C with a nonzero radius ($a^\dagger > 0$). The "pulloff" at $F^\dagger$ occurs under fixed load when $dF/da \to \infty$ or $da/dF = 0$. The branch CD with $dF/da < 0$ is physically inaccessible under fixed load, because $F^\dagger$ is already the minimum force along this curve, but possible under displacement control or fixed grips. The contact shrinks further along CD (*dark curve*). At D, the contact is reduced to a point with $a = 0$ and the solid resumes its spherical shape. Along DO, the sphere is readily out of intimate contact with the substrate, but the meniscus turns into a water bridge still exerting a traction on the sphere. Increasing tension reduces the bridge width until it breaks at O, the sphere then completely breaks free from the substrate at $F^{\dagger\dagger} = 0$. Point O is coined "pulloff" under fixed grips. The detachment trajectory is similar for other moisture level. In the dry conditions with RH $\approx$ 0%, $r_k \to 0$, $p^* \to \infty$, the cohesive zone vanishes, and a large pulloff force $|F^\dagger|$ is predicted due to a constant γ. As RH increases, $|F^\dagger|$ approaches the limit of $F^\dagger = -4\pi R\gamma$ along CD (*gray curve*) and $a^\dagger$ approaches zero, which are summarized in Fig. 2. It is noted that the model fails when $2r_k$ is of the same order of magnitude as R.

Figure 2(*b*) shows $F(\delta)$ for a range of RH. For RH = 5%, δ is nonzero at $F = 0$ due to adhesion (not shown). Applied tension ($F < 0$) further reduces δ until "pulloff" under fixed load occurs at C with maximum tensile load with $dF/d\delta = 0$. Under fixed grips, δ can decrease further under stable equilibrium. At D, $\delta = 0$ and the sphere resumes its spherical shape. Here the cohesive zone extends to the meniscus with $a_1 = 2\ (R \times r_k)^{1/2}$, and the external force to maintain equilibrium becomes $F = -F_{ad} = -p^* \times \pi\ a_1^2 = -4\pi R\gamma$. Further decrease in δ (< 0) detaches the sphere from the substrate, but the sphere is linked by a bridge to the substrate. To maintain mechanical equilibrium along DH, the applied load is balanced by the adhesion force

$$F = -F_{ad} = -p^* \times \pi a_1^2 = -4\pi R\gamma \times \left(1 + \frac{\delta}{2r_k}\right) \tag{10}$$

where $a_1 = (2R\ (\delta + 2r_k))^{1/2}$ is the bridge radius found by simple geometry. As the sphere moves further out from the substrate, the

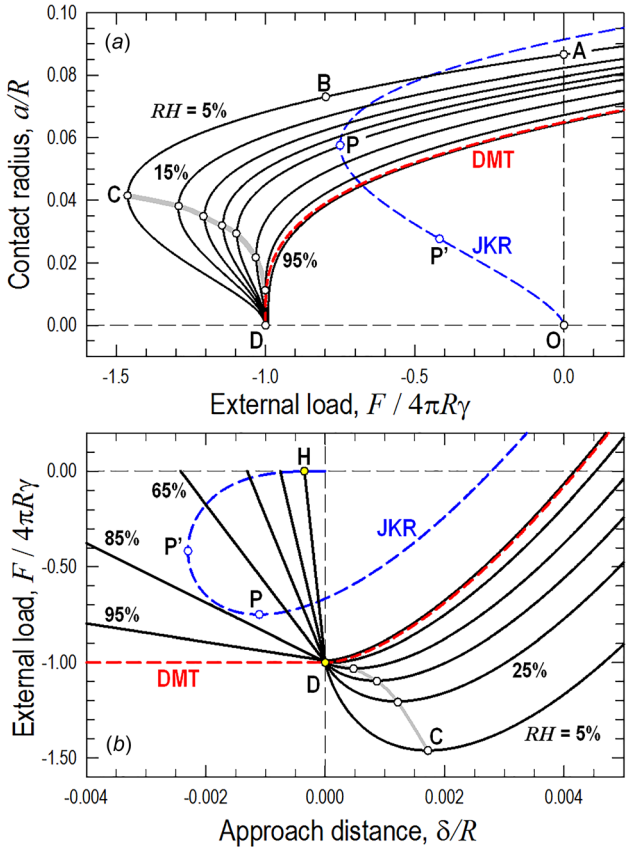

Fig. 2 Adhesion of an elastic sphere with an elastic modulus $E = 1.0$ GPa in the presence of moisture: (*a*) Contact radius as a function of applied load for RH = 5%, 15%, 25%, 35%, 45%, 65%, 85%, and 95% based on the present model (*dark curves*). At RH = 5%, external tension shrinks the contact area along ABCDO and causes "pulloff" under fixed load at C. Fixed grips continues along CD. At D, a point contact is left and "pulloff" occurs at O. The gray curve shows the locus of fixed load "pulloff". The Bradley's model is essentially the horizontal axis since contact radius is always zero. The DMT model (*red dashed curve*) is based on the surface tension of water and "pulloff" occurs at D. The JKR model (*blue dashed curve*) shows "pulloff" under fixed load at P and "pulloff" under fixed grips at P'. (*b*) Applied load as a function of approach distance for RH = 5%, 25%, 45%, 65%, 85%, and 95% based on the present model (*dark curves*). Detachment proceeds along CDH. "Pulloff" under fixed load occurs at C and under fixed grips at H. The "pulloff" locus are shown as gray curves, along with the DMT and JKR models. The Bradley's model is identical to the present model under external tension.

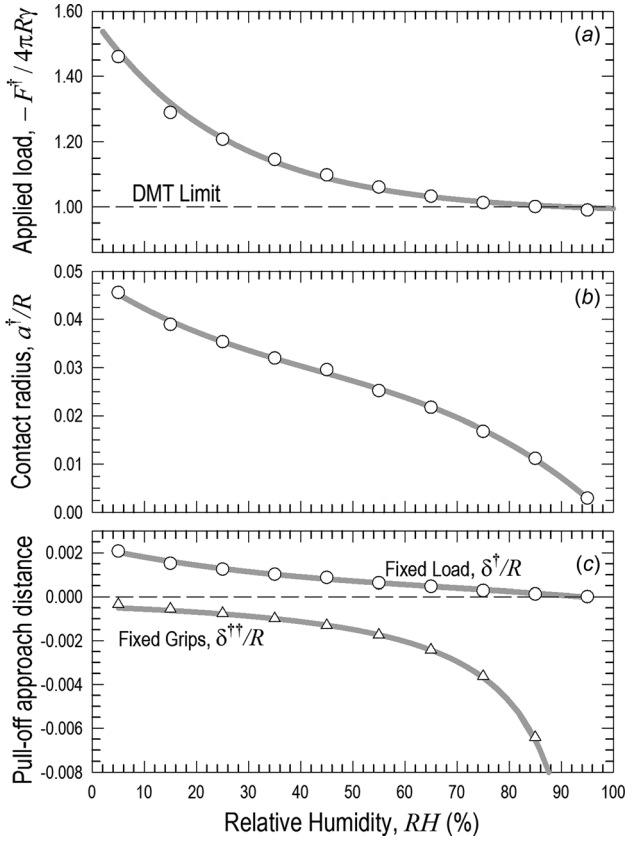

Fig. 3 "Pulloff" as a function of relative humidity: (*a*) applied tension, $-F^{\dagger}$(RH), and (*b*) contact radius $a^{\dagger}$(RH), under fixed load (c.f. gray curve CD in Fig. 2(*a*)); and (*c*) approach distance, $\delta^{\dagger}$(RH) under fixed load (c.f. gray curve CD in Fig. 2(*b*)) and $\delta^{\dagger\dagger}$(RH) under fixed grips (c.f. gray curve of negative horizontal axis in Fig. 2(*b*)).

water bridge shrinks and the external load decreases linearly with δ. At H, $\delta^{\dagger\dagger} = -2r_k$, $a_1 = 0$, the meniscus bridge collapses, the applied tension vanishes, and "pulloff" occurs at $F^{\dagger\dagger} = 0$. The fixed grips "pulloff" locus is along the negative δ-axis, corresponding to O in Fig. 2(*a*). At saturation (RH $\rightarrow$ 100%), $F^{\dagger\dagger} \rightarrow -4\pi R\gamma$ and $\delta^{\dagger\dagger} \rightarrow -\infty$ theoretically as $r_k \rightarrow \infty$ in Eq. (8). However, the water pillar collapses before δ reaches $-R$ due to the geometrical constraints.

Figure 3 shows $F^{\dagger}$, $a^{\dagger}$, and $\delta^{\dagger}$ as functions of RH. In Fig. 3(*a*), the calculated $F^{\dagger}(a = 0,\ \delta = 0)$ slightly deviates from the DMT limit of $-4\pi R\gamma$ at very high RH as the cohesive zone now extends to the sphere dimension ($a_1 \approx R$), and the Hertz assumption breaks down. Figure 3(*b*) shows the expected monotonic decreasing function of $a^{\dagger}$ (RH) that approaches $a^{\dagger} = 0$ in saturated moisture. Figure 3(*c*) shows $\delta^{\dagger}$ (>0) under fixed load and $\delta^{\dagger\dagger}$ (<0) under fixed grips as RH varies. A drastic decrease in $\delta^{\dagger\dagger}$ is expected as RH exceeds 50% since the large meniscus (r_k) sustains a long water bridge (c.f. Eq. (8)).

4 Discussion

The new model is rigorously compared with the classical adhesion models: (i) Bradley's model [1] where the sphere is rigid and nondeformable, (ii) DMT theory [19] for small but stiff spheres in the presence of a weak force with an ideal infinite range, and (iii) the JKR theory [20] for large but soft spheres in the presence of a strong surface attraction with an ideal zero range.

In Bradley's model, a rigid sphere makes only a single point contact with the substrate with $\delta = 0$ and $a = 0$ independent of both RH and F. In the presence of a meniscus, the sum of the applied load and Laplace pressure is balanced by the reaction force at the point contact in the form of a delta function such that the adhesion force is a constant with $F_{ad} = 4\pi R\gamma$ for $F \geq 0$. When δ turns negative, the sphere is out of intimate contact with the substrate but is linked by a water pillar. Equation (10) holds, and the behavior is identical to the present model. Pulloff occurs when the water pillar breaks.

In the classical JKR model [12], the disjoining pressure is taken to be infinite with a vanishingly small force range though the energy to bring the two adhering surfaces together is finite. The tensile stress at the contact edge is therefore theoretically infinite and is capable of deforming the sufficiently soft sphere to the Griffith parabola with $(\partial y/\partial r)_{r=a} \rightarrow \infty$. An energy balance predicts "pulloff" under fixed load at P in Fig. 2, where $F^{\dagger} = -3\pi R\gamma$, $a^{\dagger} = (9\pi R^2\gamma \quad (1-\nu^2)/4E)^{1/3}$, and $\delta^{\dagger} = -(a^{\dagger})^2/3R$, whereas "pulloff" under fixed grips occurs at P' where $F^{\dagger\dagger} = -(5/12)\pi R\gamma$, $a^{\dagger\dagger} = (\pi R^2\gamma\ (1-\nu^2)/4E)^{1/3}$, and $\delta^{\dagger\dagger} = -3(a^{\dagger})^2/R$. A close examination of these underlying assumptions prompts one to check for limitations. Laplace pressure cannot increase indefinitely but has

an upper bound of the hydrogen bonds of water in the molecular scale or vapor pressure in the macroscopic scale. It is unable to deform a sufficiently stiff sphere (e.g., silica glass) to the ideal parabolic shape at the contact edge, since hydrogen bonds will be broken and water molecules dissociate beforehand. The present model predicts $a^\dagger > 0$ under fixed load, but since there is no local deformation at the contact edge as in JKR. Both $F^\dagger$ and $a^\dagger$ are distinctly different from the JKR values. It is noted that Hertz contact theory in Eqs. (1)–(3) is adopted in this work for stiff solid sphere. Should a large and soft sphere be considered, the deformed profile will significantly deviated from Hertz, and a better computational model (e.g., Refs. [6] and [12]) will be necessary for the thermodynamic energy balance.

The present model is similar to the DMT model to some extent; in that, the sphere deforms according to the Hertz theory, and the adhesion mechanics serves as the limit for RH approaching saturation as shown in Fig. 2(*b*). Maugis's version of DMT assumes an infinite force range [21] and $a_1 \to \infty$. "Pulloff" under fixed grips occurs at $\delta \to \infty$, and the external tension to maintain the infinite water pillar remains constant at $F^\dagger = -4\pi R\gamma$ for all $\delta \le 0$. In the absence of sphere–substrate interaction, the "crack front" is located literally at the meniscus, which is consistent with the classical experiment in measuring surface tension of a liquid trapped between two cantilevers [10,11]. One interesting implication of DMT is that the water molecules must penetrate all the way from the meniscus $z(r = a_1) = 2r_k$ to the contact edge at $z(r = a) = z_0$ so that the Laplace pressure is present in the entire stretch of the cohesive zone. In reality, the physical dimension of two water molecules bonded by a typical hydrogen bond is roughly 8.4 Å. A *vacuum* thus exists between the contact edge and the molecular wedge, or, $p = 0$ in $r(z_0)$ to $r(z = 8.4$ Å). In the limit of RH = 100%, $a_1 \gg r(z = 8.4$ Å), and our model approaches DMT.

In the intermediate range of RH, the new model requires the Laplace pressure to be bounded by the cohesive zone, $p = p^*$ in $r(z = 8.4$ Å) to $r(z = 2r_k)$. Based on Eq. (8), $2r_k = 8.4$ Å at RH ≈ 30%, and no meniscus can exist below this critical RH. The corresponding Laplace pressure is too weak to deform the contact edge to the Griffith parabola. The contact edge can now be arbitrarily chosen to be in the small range between $r(z_0)$ to $r(z = 8.4$ Å). Without loss of generality, we choose to assume the Hertzian compressive stress within the contact circle and the Laplace pressure without, regardless the exact location of the contact edge. To further justify the new model, Fig. 4 shows the deformed profile for $E = 10$ GPa and a range of RH according to Maugis's cohesive zone model along with the JKR and DMT limits. All curves show a characteristic kink, where the slope $\partial z/\partial r$ changes abruptly indicating the cohesive zone edge $r = a_1$. At RH < 30%, $2r_k < 8.4$ Å and intersurface force does not exist. Therefore, meniscus alone is unable to lead to the JKR limit. In Maugis's calculation, the compressive contact stress gradually turns tensile radially outward and reaches the maximum tension matching the Laplace pressure. However, the absence of intrinsic solid–solid interaction and the finite water molecular dimension do *not* allow tension within the contact. Our model allows a discontinuity in stress at the contact edge where it abruptly drops from zero based on Hertz to the full strength of Laplace pressure.

It is worthwhile to mention a few existing models in the literature. Christenson [5] measured an *increasing* pulloff force as RH rises as shown in Fig. 5. The ostensible contradiction seems to be explainable by the van der Waals attraction at the solid–solid interface that is inevitable and overshadows the Laplace pressure. Xue and Polycarpou [14] used a numerical approach to show $F^\dagger$ as a monotonic *decreasing* function of RH > 70% that approaches the DMT limit at saturated moisture. Such results match with the present model quite well, though Polycarpou only focused on the wet environment with RH > 70% only to avoid the intrinsic solid–solid interaction. We calculated the data points for RH < 70% based Polycarpou's data and Maugis' model as suggested by Xue and Polycarpou [14], which do not match quite well with the present model. Based on the JKR model, Fogden and White [8] predicted the large and soft spheres at relatively low RH pull off at $F^\dagger \to -3\pi R\gamma$, shown in the Fig. 5. The size of water molecule was not considered in their model. In the presence of a strong sphere–substrate interaction, the meniscus becomes negligible, and the adhesion–detachment mechanics approaches the JKR limit, which is the beyond the scope of this work. Another set of data and theoretical model worth discussion is that due to Grobelny et al. [9]. The capillary force, equivalent to F_{ad} (a) in Eq. (7), is deduced based on the Kelvin radius, Laplace pressure, and Hertz contact theory, and serves as the critical threshold for pulloff. However, the *repulsive* reaction force at the contact is altogether ignored, or equivalently, $F_H = 0$ in Eq. (5) and $F^\dagger = F_{ad}$. Since the force balance is offset, the mechanical response $F(a,\delta)$ and the subsequent $F^\dagger$ and $F^{\dagger\dagger}$ are different from the present work. Despite such inconsistencies, the experimental

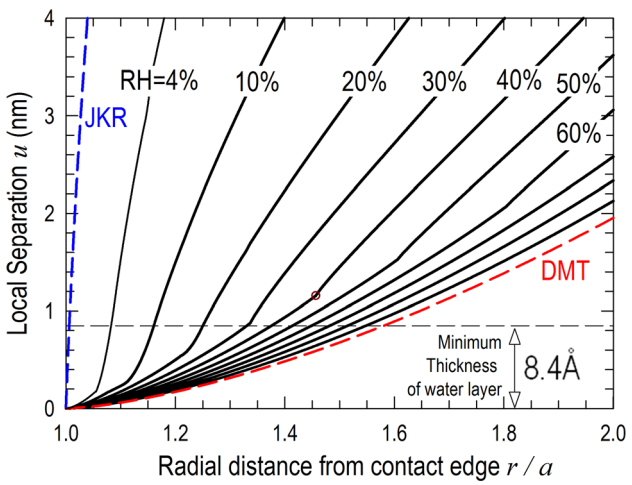

Fig. 4 Deformed profile at the contact edge exposed to moist air in the absence of an applied load $F = 0$. Minimum thickness of liquid water is set to be 8.4 Å (*dashed line*). At RH = 40%, the profile changes abruptly at the circle marked, indicating the meniscus or cohesive zone edge. The JKR and DMT limits are shown as dashed curves.

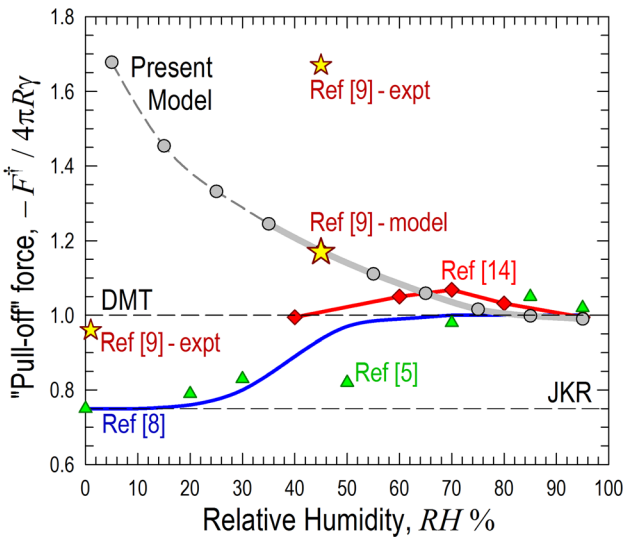

Fig. 5 "Pulloff" force under fixed load as a function of relative humidity, showing the present model (*solid curve* for RH > 30% and *dashed curve* for RH < 30%), theoretical results from Refs. [8], [9], and [14], measurements from Refs. [5] and [9]. Note that the two experimental data at RH = 0% and 45% from Ref. [9] neither fall into the main trend of this work and others nor match with the theory from the same paper.

data in Ref. [9] are presented for gold microsphere with $E_{gold} \approx 78$ GPa, which deviate significantly from trends in this work and others. However, the theoretical model for RH = 45% coincides with our model.

The classical Tabor parameter, $\mu \propto (R\ \gamma^2/E^2\ z_0^2)^{1/3}$ or $(R\ p^{*2}/E^2)^{1/3}$, and its various forms, are used to discuss the JKR to DMT transition in the literature such that small μ leads to DMT-limit and large μ to JKR-limit [6,7,22,23] including pulloff force as a function of RH. In this work, μ is not an appropriate parameter, because the deformed geometry of the sphere is established solely on the classical Hertz contact theory (c.f. Eq. (4)), and the local deformation at the contact edge similar to the JKR model is ignored. A comprehensive model will have to solve the mathematically involved governing solid mechanics equations, which is beyond the scope of this paper. For stiff sphere like silica and glass, a full-fledged computation unlikely leads to a deformed geometry significantly different from the Hertz model. This work aims to demonstrate how a proper description of the Laplace pressure leads to an adhesion mechanics distinctly different from the classical JKR and DMT model.

As a final remark, implications of the new model is significant. For instance, it is known that heating and drying helps preventing coagulation in powder (e.g., glass beads, dry spray) and stiction in microdevices. This work shows that once RH drops to roughly 30%, water condensation, and the consequent adhesion in glass become relatively unimportant.

5 Conclusion

A simple adhesion model is derived for an elastic sphere adhering to a rigid planar substrate in the presence of moisture. The model is useful in discussing adhesion of microscopic objects, and the derived values of "pulloff" force and contact radius can be used to deduce the magnitude and range of intersurface forces. Contrary to the classical description based on Maugis's JKR–DMT transition, meniscus alone causes $|F^{\dagger}|$ to exceed $2\pi R\gamma$ for any relative humidity and the DMT limit only holds at saturation.

Acknowledgment

This work was supported by National Science Foundation. Any opinions, findings, and conclusions or recommendations expressed in this material are those of the authors and do not necessarily reflect the views of the National Science Foundation.

Funding Data

- Directorate for Engineering (CMMI No. #1333889).

References

[1] Kendall, K., 2001, *Molecular Adhesion and Its Application: The Sticky Universe*, Kluwer Academic/Plenum Publishers, New York.
[2] Johnson, K. L., 1985, *Contact Mechanics*, Cambridge University Press, Cambridge.
[3] Jones, R., Pollock, H. M., Cleaver, J. A. S., and Hodges, C. S., 2002, "Adhesion Forces Between Glass and Silicon Surfaces in Air Studied by AFM: Effects of Relative Humidity, Particle Size, Roughness, and Surface Treatment," Langmuir, **18**(21), pp. 8045–8055.
[4] Christenson, H. K., 1985, "Capillary Condensation in Systems of Immiscible Liquids," J. Colloid Interface Sci., **104**(1), pp. 234–249.
[5] Christenson, H. K., 1988, "Adhesion Between Surfaces in Undersaturated Vapors—A Reexamination of the Influence of meniscus Curvature and Surface Forces," J. Colloid Interface Sci., **121**(1), pp. 170–178.
[6] Maugis, D., and Gauthier-Manuel, B., 1994, "JKR–DMT Transition in the Presence of a Liquid meniscus," J. Adhes. Sci. Technol., **8**(11), pp. 1311–1322.
[7] Xu, D., Liechti, K. M., and Ravi-Chandar, K., 2007, "On the Modified Tabor Parameter for the JKR–DMT Transition in the Presence of a Liquid meniscus," J. Colloid Interface Sci., **315**(2), pp. 772–785.
[8] Fogden, A., and White, L. R., 1990, "Contact Elasticity in the Presence of Capillary Condensation: 1. The Nonadhesive Hertz Problem," J. Colloid Interface Sci., **138**(2), pp. 414–430.
[9] Grobelny, J., Pradeep, N., Kim, D.-I., and Ying, Z., 2006, "Quantification of the Meniscus Effect in Adhesion Force Measurements," Appl. Phys. Lett., **88**(9), p. 091906.
[10] Wan, K.-T., and Lawn, B. R., 1990, "Surface Forces at Crack Interfaces in Mica in the Presence of Capillary Condensation," Acta Metall. Mater., **38**(11), pp. 2073–2083.
[11] Wan, K.-T., Smith, D. T., and Lawn, B. R., 1992, "Fracture and Contact Adhesion Energies of Mica-Mica, Silica-Silica and Mica-Silica," J. Am. Ceram. Soc., **75**(3), pp. 667–676.
[12] Maugis, D., 2000, *Contact, Adhesion and Rupture of Elastic Solids*, Springer, New York.
[13] Zeng, J., and Streator, J. L., 2003, "A Micro-Scale Liquid Bridge Between Two Elastic Spheres: Deformation and Stability," Tribol. Lett., **15**(4), pp. 453–464.
[14] Xue, X., and Polycarpou, A. A., 2008, "Meniscus Model for Noncontacting and Contacting Sphere-on-Flat Surfaces Including Elastic–Plastic Deformation," J. Appl. Phys., **103**(2), p. 023502.
[15] Xue, X., and Polycarpou, A. A., 2007, "An Improved Meniscus Surface Model for Contacting Rough Surfaces," J. Colloid Interface Sci., **311**(1), pp. 203–211.
[16] Wan, K.-T., and Lawn, B. R., 1992, "Effect of Chemical Interaction on Barenblatt Crack Profiles in Brittle Solids," Acta Metall. Mater., **40**(2), pp. 3331–3337.
[17] Hertz, H., 1896, *Miscellaneous Papers*, Macmillan, London.
[18] Johnson, K. L., and Greenwood, J. A., 2008, "A Maugis Analysis of Adhesive Line Contact," J. Phys. D: Appl. Phys., **41**(5), p. 199802.
[19] Derjaguin, B. V., Muller, V. M., and Toporov, Y. P., 1975, "Effect of Contact Deformations on the Adhesion of Particles," J. Colloid Interface Sci., **53**(2), pp. 314–326.
[20] Johnson, K. L., Kendall, K., and Roberts, A. D., 1971, "Surface Energy and the Contact of Elastic Solids," Proc. R. Soc. London A, **324**(1558), pp. 301–313.
[21] Maugis, D., 1992, "The JKR–DMT Transition Using a Dugdale Model," J. Colloid Interface Sci., **150**(1), pp. 243–269.
[22] Wan, K.-T., and Julien, S. E., 2009, "Confined Thin Film Delamination in the Presence of Intersurface Forces With Finite Range and Magnitude," ASME J. Appl. Mech., **76**(5), p. 051005.
[23] Li, G., and Wan, K.-T., 2010, "Parameter Governing Thin Film Adhesion-Delamination in the Transition From DMT- to JKR-Limit," J. Adhes., **86**(10), pp. 969–981.